

# Removal of Pb (II) from aqueous solution using hydrotalcite-like nanostructured material

Katlego Setshedi, Jianwei Ren, Ochieng Aoyi and Maurice Stephen Onyango

Department of Chemical and Metallurgical Engineering, Tshwane University of Technology, Pretoria, South Africa.  
Department of Chemical Engineering, Vaal University of Technology, South Africa.

Novel nanostructured hydrotalcite (HT) adsorption medium was prepared and its ability to remove Pb(II) from aqueous solution was demonstrated. The media was characterized using Fourier transform infrared spectroscopy (FTIR), X-ray diffraction (XRD), transmission electron microscope (TEM) and Thermogravimetric Analysis (TGA). Batch adsorption was chosen in which changes in solution pH, initial concentration and temperature were the main variables. In addition, the adsorption of Pb(II) in binary component systems was explored. Results reveal that Pb(II) adsorption was rapid and favoured at increased temperature and pH. It was observed, in comparison with single component system (Pb only), that the presence of co-ions reduces the Pb(II) adsorption suggesting a competitive adsorption at the water-hydrotalcite (HT) interface. The kinetic data fitted well to Ho pseudo second order model while the equilibrium data were satisfactorily described by the Langmuir isotherm. The Langmuir maximum adsorption capacity of Pb(II) at pH 6.0 was found to be 333 mg/g at 298 K and 500 mg/g at 308 K and 318 K. From the uptake values, this study reveals that nanostructured HT is an effective adsorbent for the removal of Pb(II) from aqueous solutions.

**Key words:** Adsorption, nano-hydrotalcite, Pb(II) ions, equilibrium, kinetics.

## INTRODUCTION

Water contamination, reported by the World Health Organization (WHO), is responsible for more than 3.5 million deaths per year worldwide, and heavy metals pollution makes the situation worse due to their immense toxicity and non-biodegradability (Pronczuk et al., 2011; Jayakumar et al., 2010). Heavy metal ions can be accumulated through the food chain even at lower concentrations, leading to reduced mental and central nervous function, lower energy levels and damaged blood composition, lungs, kidneys, liver and other vital organs (Ozdes et al., 2009). Lead in wastewater comes mainly from the discharge of battery manufacturing, printing, dyeing, lead-based paint, household dust and food containers (Ekpo et al., 2008). Lead is an important compound used as an intermediate in the processing industries, which however has been recognized to be

acutely toxic to human beings when present in high amounts in water. Studies have shown that young children, infants and pregnant women are particularly susceptible to unsafe Pb(II) levels. For adults, increased levels of Pb(II) have been linked to high blood pressure and damaged hearing. Drinking, eating, inhaling even at low level of Pb(II) can cause other serious health effects (Adelekan and Abegunde, 2011; Kabbashi et al., 2009). The permissible limit of Pb(II) in drinking water and surface water intended for drinking, as set by European Union (EU), United States Environmental Protection Agency (USEPA) and WHO, are 0.010, 0.015 and 0.010 mg/L, respectively (Lalhruaitluanga et al., 2010; Li and Wang, 2009). The removal of Pb(II) contaminant from aqueous waste streams has drawn an increasing attention in the past decade due to global awareness of the underlying detrimental effect to health and the environment.

Several conventional methods such as chemical precipitation, ion-exchange, electro flotation, membrane filtration, reverse osmosis have been employed to remove

---

\*Corresponding author. E-mail: OnyangoMS@tut.ac.za. Tel: +27 12 382 3533. Fax: +27 12 382 3532.

Pb(II) from water (Naiya et al., 2009; Naeem et al., 2009; Ricordel et al., 2010; Heier et al., 2010; Dialynas and Diamadopoulou, 2009). These techniques are either costly or have significant disadvantages such as generation of metal bearing sludge or wastes, incomplete metal removal, and the requirement of disposal of secondary wastes. Adsorption is considered quite an eco-effective purification and separation technique used in wastewater treatment over the last few decades. In recent years, various adsorbents have been used for the removal of Pb(II) from aqueous solution, and the efficiency of adsorption depends on many factors, such as the surface area, pore size distribution, polarity, and functional groups of the adsorbent (Anwar et al., 2010; Amarasinghe and Williams, 2007; Diouf et al., 2011; Egila et al., 2011; Özer, 2007; Singh et al., 2008; Singh et al., 2008; Xu et al., 2008; Tao et al., 2009). Adsorption technique though robust in nature, suffers from massive mass transport resistance due to the size of the adsorbents. This limitation can be overcome through the use of nanotechnologically engineered materials (nanomaterials). Nanomaterials are attractive because they can exhibit an array of novel properties such as large surface area, potential for self assembly, high specificity, high reactivity, catalytic potential, and absence of internal diffusion resistance, which are promising to develop new or improve existing technologies in wastewater treatment (Zhang et al., 2006). Some studies were recently reported in literature on the removal of Pb(II) from water using synthesized nanomaterials, such as kaolin supported nanoscale zero-valent iron (Zhang et al., 2010), nano-TiO<sub>2</sub> matrix (Li et al., 2009) and carbon nanotubes (Rupareila et al., 2008).

Layered double hydroxides (LDHs), also known as hydrotalcites (HT) or anionic clays, have also been explored for amelioration of wastewater containing heavy metals. Hydrotalcites (HT) can be described by the general formula  $[M_{1-x}^{2+}M_x^{3+}(\text{OH})_2]^{x+} [A_{x/n}^{n-} \cdot m\text{H}_2\text{O}]^{x-}$  where M<sup>2+</sup> and M<sup>3+</sup> are divalent and trivalent metal cations, respectively. The structure consists of brucite-like layers with a positive charge owing to the replacement of Mg<sup>2+</sup> by Al<sup>3+</sup>, this charge being balanced by interlayer anions (A<sup>n-</sup>). HTs have large ionic exchange capacity of 3.3 meq/g in comparison to 1 meq/g in cationic clays (Carriazo et al., 2007). Furthermore, the ability of the HT to recover its structure on heating up to the range of 500 to 800°C makes them attractive materials, as the calcined product has a memory effect and therefore it is possible to reconstruct the original structure, which in turn provides the potential for reuse and recycle of the adsorbent (Anirudhan and Suchithra, 2008). However, there is no report on the use of nano-scale HT in Pb(II) removal from aqueous solutions.

Consequently, in this study, the Pb(II) adsorption characteristics of nano-scale hydrotalcite-like media were investigated by using a batch sorption mode. The effect of temperature, pH, competitive ions and initial

concentration were studied, with the aim to determine the sorption rate and capacity of hydrotalcite-like nanoparticles for Pb(II).

## MATERIALS AND METHODS

### Materials

Reagent grade chemicals such as NaOH, HNO<sub>3</sub> (Sigma Aldrich) and various salts of polyvalent metals were used as required. Water samples contaminated with heavy metal were prepared using their respective metal ion salts.

### Preparation and characterization of adsorption media

The nano-scale hydrotalcite-like (HT) samples were synthesized following the standard aqueous precipitation method of Reichle et al. (1986) under a bubbling constant flow of nitrogen in the reaction medium and vigorous stirring. 100 ml of an aqueous solution of Mg(NO<sub>3</sub>)<sub>2</sub>·6H<sub>2</sub>O (0.75 mol) / Cr(NO<sub>3</sub>)<sub>3</sub>·9H<sub>2</sub>O (0.25 mol) and an aqueous solution of NaOH(0.5 M) / Na<sub>2</sub>CO<sub>3</sub> were added drop wise together in such a way that the pH remained at a constant value of 10.5. The resulting solids were aged at 65°C for 14 h, washed three times with deionized water and dried at 110°C overnight.

The morphology of the nanoparticles sample was studied using transmission electron microscope (TEM) (JEOL JEM-100S). The TEM specimens were prepared by putting a drop of dilute suspensions of the nanoparticles in 2-propanol on a copper grid. To investigate the functional groups before adsorption, specimens were studied by using a Fourier transform infrared spectroscopy (FTIR). The FTIR spectra were recorded using KBr pellets with slow scan and normal slit width. FTIR characterization can be used to identify the presence of the charge balancing anion in the interlayer, the type of bonds formed by the anions and their orientations (Goh et al., 2008).

Information about the crystal structure and crystallite size before and after adsorption was achieved by characterization with the Panalytical X'pert PRO PW 3040/60 X-ray diffractometer with a Cu Kα (λ = 0.154 nm) monochromated radiation source operated at 45.0 kV and 40.0 mA. XRD data was collected in the 2θ ranging from 5 to 160° with a step size of 0.02°. The thermal stability of the HT nanoparticles was achieved through analysis by the thermo gravimetric analyzer at temperatures ranging from 0 to 900°C.

### Batch adsorption kinetics

The experiment was carried out in a 1 L batch reactor with an initial Pb(II) concentration of 90.75 mg/L. The adsorbent mass was fixed at 0.1 g. The reactor was stirred with an overhead stirrer operated at 200 rpm. At predetermined time intervals, 10 ml samples were taken from the reactor, filtered through a syringe filter and residual Pb(II) concentration was measured by an atomic absorption spectrophotometer (AAS). By performing appropriate material balance, the quantity of Pb(II) adsorbed at the selected time intervals was determined and used for kinetic analysis. Amounts of Pb(II) ions adsorbed at any time were calculated by,

$$q_t = \frac{V(C_o - C_t)}{m} \quad (1)$$

where C<sub>o</sub> (mg/L) is the initial concentration, C<sub>t</sub> (mg/L) the concentration at any time, q<sub>t</sub> (mg/g) the amount of Pb(II) adsorbed at any time, m (g) the adsorbent mass and V (L) is the solution volume.

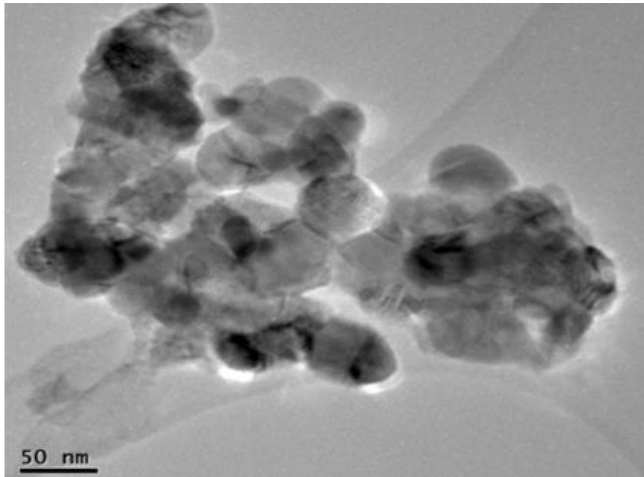


**Figure 1.** Transmission electron microscope (TEM) image of the HT nanoparticles.

#### Effect of temperature

Sorption isotherm data were generated by contacting 0.05 g of sorption media with a Pb(II)-containing aqueous solution. 50 ml sample of Pb(II) ranging from 100 to 400 mg/L were pipette into 100 ml plastic bottles. The bottles were then placed in a thermostatic shaker and shaken for 24 h at 298, 308 and 318K. The shaking speed was set at 200 rpm. At the end of the experiment, samples were withdrawn from the test bottles and filtered through syringe filters and the residual Pb(II) concentration was measured by an atomic absorption spectrophotometer (AAS). The equilibrium sorption capacity was determined from Equation 2.

$$q_e = \frac{V(C_o - C_e)}{m} \quad (2)$$

where  $q_e$  (mg/g) and  $C_e$  (mg/L) are the amount of Pb(II) adsorbed and the equilibrium concentration, respectively.

#### Effect of pH

The effect of pH was studied by varying the initial pH of the Pb(II) solution within the range of 1 to 8, using either NaOH or HCl. Accordingly, adsorption was done by adding 0.05 g of the HT nanoparticles to 50 ml of 400 mg/L Pb(II) solution contained in plastic bottles. The bottles were placed in a thermostatic shaker and shaken for 24 h. The samples were then filtered and the residual Pb(II) concentration was measured with the AAS.

#### Effect of co-existing ions

The effect of co-existing ions was explored in binary components systems. It is well known that most industrial wastewaters contain several species of metals, not a single component, and so the metallic sorption behaviours become more complicated than in single-component system. Thus, a sorption research for multiple metals is more realistic than for a single metal system. The considered co-existing ions were of nickel (Ni) and cobalt (Co). Experiments were carried by mixing 400 mg/L of Pb(II), Co(II) and Ni(II) ions at a molar ratio of 1:1, and then 50 ml of the sample was

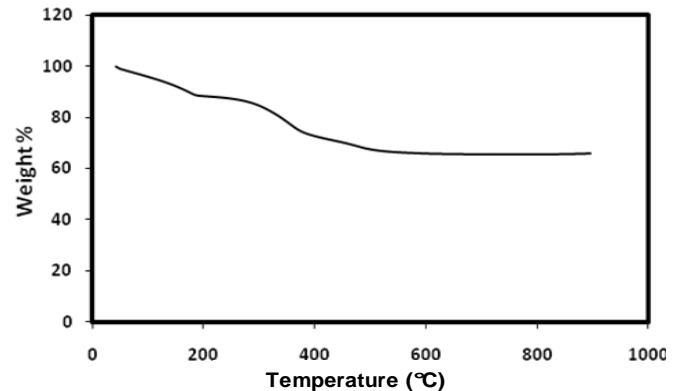


**Figure 2.** Thermogravimetric analysis of the HT nanoparticles.

contacted with 0.05 g of the HT nanoparticles for 24 h and then filtered. The residual concentration was determined by the AAS. By carrying appropriate material balance, the quantity of Pb(II) adsorbed was determined.

## RESULTS AND DISCUSSION

### Characterization

The transmission electron microscope (TEM) image of a typical HT nanoparticles used in this study is shown in Figure 1. TEM analysis offers a closer look at the morphological features of the material. The TEM micrographs of the HT nanoparticles show hexagonal round edged form crystals related to brucite sheets. The particles exist as agglomerates and are approximately 50 nm in size. Under nanotechnology, the acceptable size limitation is in the range 1 to 100 nm. Hence, hydrotalcite prepared in this study qualifies as nanostructured material.

The thermal stability of the HT sample was studied and is shown in Figure 2. The three steps weight losses of the HT sample are observed between room temperature and 500°C. In the first step, we observe only 11% decomposition of the HT nanoparticles. The initial weight loss is due to the removal of adsorbed water in the interlayer region. The second and the third weight losses are observed between 300 and 500°C, attributable to the decomposition of the carbonate ions as well as dehydroxylation of the interlayer anions (Mokhtar et al., 2010). It is unlikely to find adsorption being carried out above such temperatures. Thus the HT nanoparticles can be considered to be thermally stable.

The FTIR analysis of HT materials gives important information about the anions existing in the interlayer between the brucite-like sheets. The FTIR spectrum of the HT is shown in Figure 3. The broad band observed in the HT spectrum in the 3400 to 3600  $\text{cm}^{-1}$  range is due to the vibration of structural  $\text{OH}^-$  groups from the brucite-like layers. The bending vibration of the interlayer water

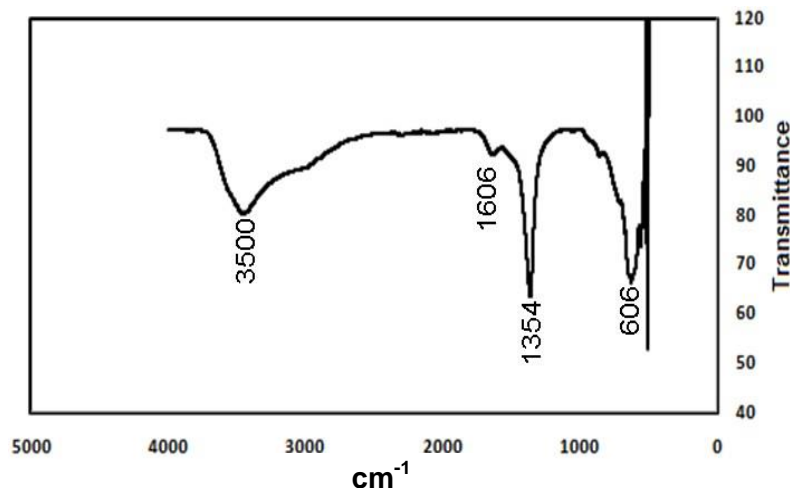


**Figure 3.** FTIR spectra of the HT nanoparticles.

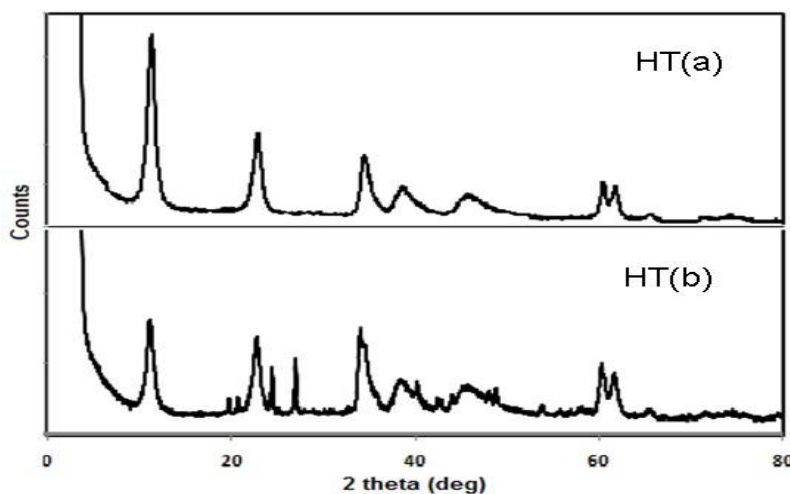


**Figure 4.** XRD analysis of the HT nanoparticles before (a) and after  $\text{Pb(II)}$  adsorption (b).

occurs at 1606  $\text{cm}^{-1}$ . The bands observed at approximately 1354 and 606  $\text{cm}^{-1}$  may be assigned to carbonate ions. Goh et al. (2008) observed similar results when they studied the application of layered double hydroxides for the removal of oxyanions.

The XRD analysis of the HT nanomaterial before and after  $\text{Pb(II)}$  adsorption is shown in Figure 4. Peaks at 11.5, 23.0 and 34.7° are similar to typical peaks found in layered double hydroxide (24). The typical X-ray patterns of LDHs, contain sharp basal reflections at low  $2\theta$  values corresponding to successive orders of basal spacing, but weak and non basal at high  $2\theta$  angle (Goh et al., 2008). Moreover, the XRD patterns of the prepared HT used in this study present sharp and symmetric peaks for (003), (006), (009), (110) and (113) and broad, less intense and

asymmetric reflections for the non-basal (012), (015) and (018) planes. The reflection patterns in the HT sample were also identified by previous reports (Mokhtar et al., 2010). Overall, a change in peak intensities after  $\text{Pb}^{2+}$  adsorption towards lower values is observed around 11.5, 23.0, 34.7 and 39.2° in the  $2\theta$  degree suggesting a bonding interaction between the HT nanoparticles and  $\text{Pb(II)}$  ions. Moreover, new peaks at 24.5 and 27.0° were observed.

### Effect of pH

The effect of pH on the adsorption of  $\text{Pb(II)}$  is presented in Figure 5. The pH of the aqueous solution is an

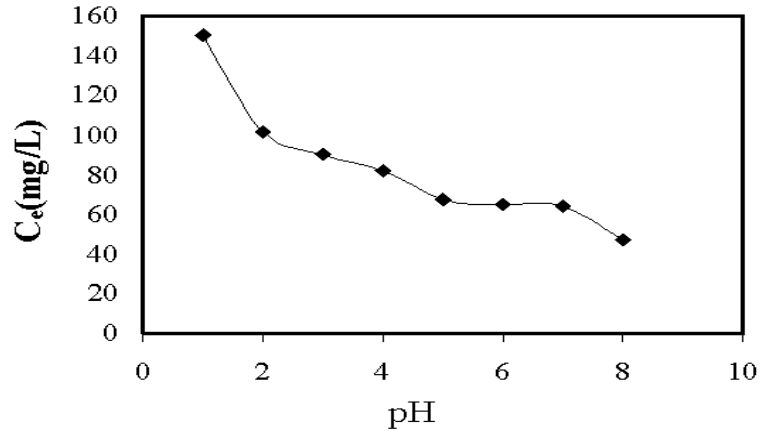


Figure 5. Effect of pH on Pb(II) adsorption onto HT nanoparticles.

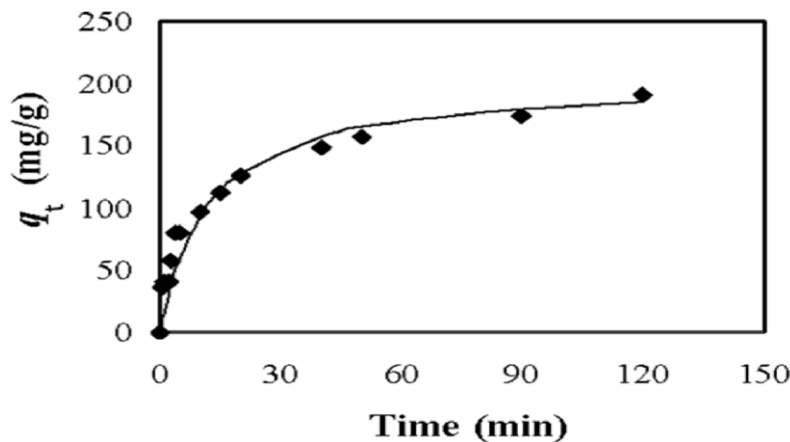


Figure 6. Adsorption kinetics of Pb(II) ions onto HT nanoparticles.

important operational parameter in the adsorption process because it affects the solubility of the metal ions, concentration of the counter ions on the functional groups of the adsorbent and the degree of ionization of the adsorbate during reaction (Amuda et al., 2007). The active sites on an adsorbent can either be protonated or deprotonated depending on the pH while at the same time the adsorbate speciation in solution depends on the pH too. Lead for example exists as  $Pb^{2+}$ ,  $PbOH^+$  and  $Pb(OH)_3^-$  depending on pH. As observed in Figure 5, the residual Pb(II) ions gradually decrease from low pH to high pH. This implies that the metal ion uptake was increased with an increase in solution pH. At low pH, there is competitive adsorption between  $H^+$  and  $Pb^{2+}$  ions on the hydroxyl surface. At high pH values, the quantity of  $H^+$  ion is reduced, Pb(II) still has a net positive charge but exists as  $PbOH^+$  while most active sites on the adsorbent are de-protonated. This enhances Pb(II) uptake. Similar results were observed by Dong et al. (2010) when they studied the removal of Pb(II) from

aqueous solution by hydroxyapatite/magnetite composite adsorbent. Therefore, the subsequent experiments were performed at pH 6 to 7.

### Adsorption kinetics

The adsorption of the Pb(II) metal ions onto HT nanoparticles as a function of contact time was investigated and data are given in Figure 6. The experiment was carried at an initial concentration of 90.75 mg/L whereby 0.1 g of sorbent was contacted with 1 L of Pb(II) aqueous solution. Adsorption was rapid in the first stage and then slowed considerably as the reaction approached equilibrium. Specifically, up to 126.73 mg/g uptake was recorded in 20 min contact time. Such a rapid uptake is indicative that the active sites on HT were readily accessible for Pb(II) adsorption. The absence of internal diffusion resistance and high surface area of the HT nanoparticles further explains the rapid uptake as

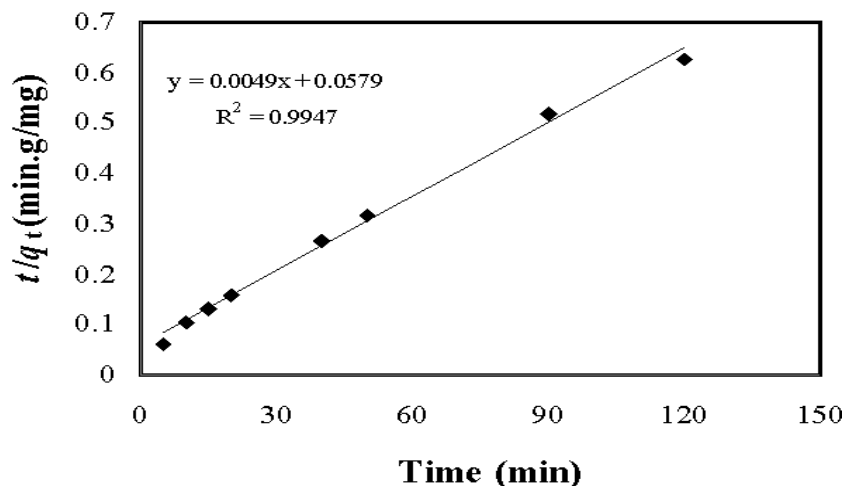


**Figure 7.** Pseudo second order kinetic plot for Pb(II) adsorption onto HT nanoparticles.

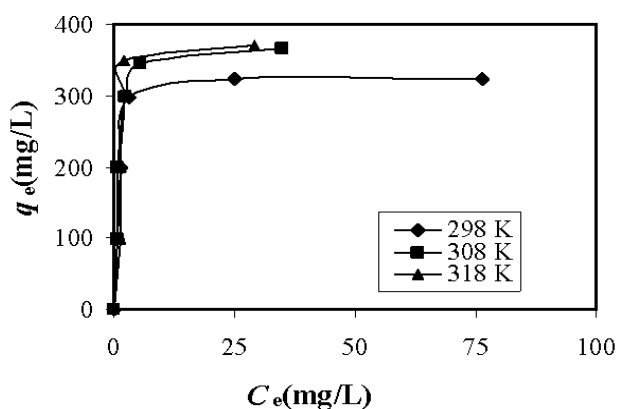


**Figure 8.** Effect of temperature on Pb(II) adsorption onto HT nanoparticles.

observed. However, there was very little increment in Pb(II) uptake after the first hour of contact because at this point, there are less vacant sites available on the adsorbent for Pb(II) sorption.

Meanwhile, to design an appropriate adsorption process, one should have sufficient information about the rate at which adsorption occurs. Thus, the kinetics of adsorption of Pb(II) ions from aqueous solution onto the HT nanoparticles were determined using the Ho and Mackay (2000) pseudo second order equation as it gave the best description of experimental data points: The linearized form of Ho's pseudo second order equation is given by;

$$\frac{t}{q_t} = \frac{1}{k_2 q_e^2} + \frac{t}{q_e} \quad (3)$$

where  $k_2$  (g/mg.min) is the rate constant of the pseudo second order equation. A plot of  $t/q_t$  versus  $t$  should be linear if the pseudo second order model is obeyed. Figure 7 shows the application of the Ho pseudo second order kinetic equation. A linear plot is obtained with an  $R^2$  value of 0.9947, suggesting that the HT-Pb(II) interaction follows the pseudo second order mechanism, thus indicating that one of the mechanisms of the adsorption of Pb(II) ions by HT nanoparticles may be by chemisorption. The calculated values of  $k_2$  and  $q_e$  are 0.00042 g/min.mg and 204 mg/g, respectively. The calculated  $q_e$  is almost similar to the experimental value and this further confirms the applicability of the Ho pseudo second order model in describing the adsorption of Pb(II) ions from aqueous solution. Many studies have reported the applicability of the pseudo second order model during lead adsorption by nanomaterials (Dong et al., 2010; Rahmani et al., 2010; Rafatullah et al., 2009; Adebawale et al., 2008).

### Effect of temperature

Temperature is known to have a profound effect on various chemical processes. Temperature affects the adsorption rate by altering the molecular interactions and the solubility of the adsorbate (Ahmaruzzaman and Sharma, 2005). The interactions between the HT nanoparticles and Pb(II) ions at 298, 308 and 318 K resulted in the Pb(II) removal from aqueous solution and are presented in the form of equilibrium data (experimental data points) as shown in Figure 8. The experimental data shows an increase in sorption capacity as temperature increases, indicating the endothermic nature of the process. For all the temperatures, the isotherms exhibit similar features: Very high uptake values in the low concentration range followed by plateau. Typically, the

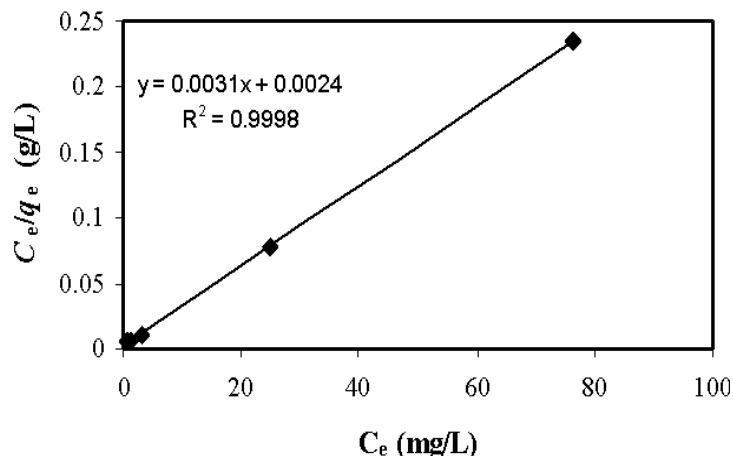


**Figure 9.** Linearized Langmuir isotherm (Equation 4) for Pb(II) adsorption onto HT nanoparticles at 298K.

**Table 1.** Langmuir and Freundlich constants at three different temperatures.

Temperature (K)	Langmuir isotherm			Freundlich isotherm		
	$q_0$ (mg/g)	$b$ (L/g)	$R^2$	$K_f$	$n$	$R^2$
298	333	1.25	0.999	160.7	5.5	0.625
308	500	1.0	0.998	175.9	3.7	0.624
318	500	1.5	0.988	183	4	0.361

isotherms show characteristics of Langmuir-type and irreversible (rectangular) isotherms suggesting high affinity of active sites for Pb(II) ion. Similar isotherm characteristic was observed by Ozay et al. (2009) in Pb(II) adsorption by magnetic hydrogels.

The Langmuir and Freundlich models were used to describe the relationship between the sorbed amount of Pb(II) and its equilibrium concentration in solution. The linearized Langmuir isotherm which is based on the monolayer sorption on the adsorbent surface with identical sorption sites is represented by the following equation,

$$\frac{C_e}{q_e} = \frac{1}{q_0 b} + \frac{C_e}{q_0} \quad (4)$$

where  $q_0$  (mg/g) is the maximum amount of Pb(II) ions per unit mass of adsorbent to form a complete monolayer on the adsorbent surface and  $b$  (L/mg) is the binding energy constant. The linear plot of  $C_e/q_e$  versus  $C_e$  at 298K is shown in Figure 9. From the plot, the Langmuir parameters were determined and are summarized in Table 1.

The  $R^2$  values of 0.999, 0.998 and 0.988 for 298, 308 and 318 K, respectively, strongly suggest that the experimental data for adsorption of Pb(II) onto HT nanoparticles fits well with the Langmuir isotherm. The

experimental data was also fitted to the Freundlich isotherm which is represented as,

$$\ln(q_e) = \ln K_f + \frac{1}{n} \ln C_e \quad (5)$$

where  $K_f$  and  $n$  are Freundlich constants related to the adsorption capacity and adsorption intensity, respectively. The parameters of the Freundlich isotherm are represented in Table 1. It is evident from the correlation coefficients of 0.625, 0.624 and 0.361 for 298, 308 and 318K, respectively, that the Freundlich isotherm did not give a good fit to the experimental data. Table 2 shows the comparison of sorption capacities of Pb(II) ion to some nanomaterials reported in literature. The maximum adsorption capacities obtained in this study are fairly attractive. It should be stressed, however, that the values given in the Table 2 originate from different studies in which the experimental conditions might not match those applied in the current study and, as such, that the comparison made here aims at showing the high uptake potential of HT nanoparticles rather than establishing a quantitative scale of efficacy among different sorbents.

### Effect of co-existing ions

Industrial discharges may contain a large number of other

**Table 2.** Comparison of the Langmuir capacity constant for Pb(II) adsorption onto other adsorbents.

Adsorbent	$q_e$ (mg/g)	Source
Nano-alumina	100	(Afkhami et al., 2010)
Nano mesoporous silica	57.74	(Heidari et al., 2009)
Mg <sub>2</sub> Al layered double hydroxide	75.18	(Zhao et al., 2011)
Magnetic carbonaceous nanoparticles	123.1	(Nata et al., 2010)
Silica-coated magnetic nanoparticles modified with $\gamma$ -MPTMS	70.4	(Huang and Hu, 2008)
Amino-functionalized Fe <sub>3</sub> O <sub>4</sub> @SiO <sub>2</sub> core-shell magnetic nanomaterial	111.78	(Wang et al., 2010)
Hydrotalcite (HT) (at 298K)	333	This work

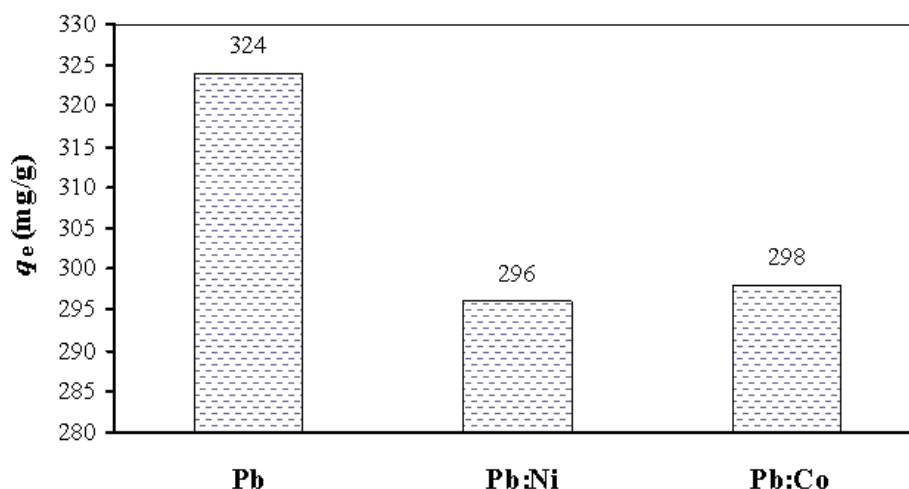


**Figure 10.** Effect of co-existing ions on Pb(II) adsorption onto HT nanoparticles.

**Table 3.** Comparison of equilibrium adsorption capacity,  $q_e$  (mg/g), for Pb (II) adsorption in single and binary component systems.

System	$q_e$ (mg/g)	$q^{\text{mix}}/q^{\circ}$
Single - Pb (II)	324	-
Binary- Pb/Ni	296	0.91
Binary- Pb/Co	298	0.91

ions which may have competitive effect on Pb(II) adsorption.

Thus, the experiment was carried in a batch mode where 0.05 g of the sorption media was contacted with 50 ml of aqueous solution containing Pb(II) ions and known quantities of commonly occurring ions in wastewater. Figure 10 shows a typical example of the adsorption of Pb in binary components of Pb/Ni and Pb/Co. It is observed that the uptake of Pb(II) ions was slightly reduced from 324 to 296 and 298 mg/g in a Pb/Ni and Pb/Co binary systems, respectively. This observation indicates that in a case of a mixture, the presence of one metal may influence, compete or exclude the recovery of another

metal from the solution. The effect of ionic interaction on the binary component sorption can be represented by the ratio of the sorption capacity for one metal ion in the presence of the other metal ion (binary component system),  $q^{\text{mix}}$ , to the sorption capacity for the same metal when it is present alone in the solution (single component system),  $q^{\circ}$ . Three case scenarios can be formulated:

$q^{\text{mix}}/q^{\circ} > 1$  the sorption is promoted by the presence of other metal ions,

$q^{\text{mix}}/q^{\circ} = 1$  there is no observable net interaction, and

$q^{\text{mix}}/q^{\circ} < 1$  sorption is suppressed by the presence of other metal ions (Kongsuwan et al., 2009).

Table 3 shows the  $q^{\text{mix}}/q^{\circ}$  from the binary components sorption of Pb (II), all of which are less than unity (0.91 for both Pb/Ni and Pb/Co binary systems). This indicates that Pb (II) sorption is suppressed by the presence of Ni (II) and Co (II) ions. However, since the  $q^{\text{mix}}/q^{\circ}$  ratio is close to 1, the suppressive effect is minimal.

## Conclusions

The removal of Pb(II) ion as a model heavy metal from

aqueous solution was carried out in a batch adsorption mode using nanostructured hydrotalcite (HT) media. The HT media exhibited effectiveness in the removal of Pb(II) ion from aqueous solutions. Higher Pb(II) uptake capacity was achieved compared with capacities of various nano-adsorbents reported in literature. The removal efficiency was controlled by solution pH, contact time, and initial temperature. Adsorption data fitted well to the Langmuir model, from which model the maximum adsorption capacity was determined as 333 mg/g at 298K. Under the influence of changes in solution pH, it was found that at pH 2 the Pb(II) removal from solution was low while a higher removal was observed as the pH increased. Kinetically, the adsorption process followed the Ho pseudo second order mechanism. While further research is being conducted, the achieved results indicate that the nanostructured HT adsorbent is a potential media for Pb(II) removal from contaminated water sources.

## ACKNOWLEDGEMENTS

This work was supported by National Research Foundation (NRF) South Africa-Romania International Science and Technology Agreements. The financial support is highly acknowledged

## REFERENCES

- Adebowale KO, Unuabonah EI, Olu-Owolabi BI (2008). Kinetic and thermodynamic aspects of the adsorption of  $Pb^{2+}$  and  $Cd^{2+}$  ions on tripolyphosphate-modified kaolinite clay. *Chem. Eng. J.*, 136(2–3): 99–107.
- Adelekan BA, Abegunde KD (2011). Heavy metals contamination of soil and groundwater at automobile mechanic villages in Ibadan, Nigeria. *Int. J. Phys. Sci.*, 6(5): 1045-1058.
- Afkhami A, Saber-Tehrani M, Bagheri H (2010). Simultaneous removal of heavy-metal ions in wastewater samples using nano-alumina modified with 2,4- dinitrophenylhydrazine. *J. Hazard. Mater.*, 181(1-3): 844- 863.
- Ahmaruzzaman M, Sharma DK (2005). Adsorption of phenols from wastewater. *J. Colloid. Interf. Sci.*, 287(1): 14-24.
- Amarasinghe BMWPK, Williams RA (2007). Tea waste as a low cost adsorbent for the removal of Cu and Pb from wastewater. *Chem. Eng. J.*, 132(1–3): 299–309.
- Amuda OS, Giwa AA, Bello IA (2007). Removal of heavy metal from industrial wastewater using modified activated coconut shell carbon. *Biochem. Eng. J.*, 36(2): 174–181.
- Anirudhan TS, Suchithra PS (2008) Synthesis and characterization of tannin- immobilized hydrotalcite as a potential adsorbent of heavy metal ions in effluent treatments. *Appl. Clay Sci.*, 42(1–2): 214–223.
- Anwar J, Shafique U, Zaman W-uz, Salman M, Dar A, Anwar S (2010). Removal of Pb(II) and Cd(II) from water by adsorption on peels of banana. *Bioresour. Technol.*, 101(6): 1752–1755.
- Carriazo D, del Arco M, Martin C, Rives V (2007). A comparative study between chloride and calcined carbonate hydrotalcites as adsorbents for Cr(VI). *Appl. Clay Sci.*, 37(3–4): 231–239.
- Dialynas E, Diamadopoulos E (2009). Integration of a membrane bioreactor coupled with reverse osmosis for advanced treatment of municipal wastewater. *Desalination*, 238(1–3): 302–311.
- Diouf R, Ndiaye SA, Muhr L (2011). Adsorption in column of Cu(II), Ni(II) and Pb(II) with XAD-7 resin impregnated with bis(2-ethylhexyl) ammonium bis(2-ethylhexyl) dithiocarbamate (BEABEDC) in aqueous solution. *Int. J. Phys. Sci.*, 6(13): 3263- 3269.
- Dong L, Zhu Z, Qui Y, Zhao J (2010). Removal of lead from aqueous solution by hydroxyapatite/ magnetite composite adsorbent. *Chem. Eng. J.*, 165(3): 827–834.
- Egila JN, Dauda BEN, Iyaka YA, Jimoh T (2011). Agricultural waste as a low cost adsorbent for heavy metal removal from wastewater. *Int. J. Phys. Sci.*, 6(8): 2152-2157.
- Ekpo KE, Asia IO, Amayo KO, Jegede DA (2008). Determination of lead, cadmium and mercury in surrounding water and organs of some species of fish from Ikpoba river in Benin city, Nigeria. *Int. J. Phys. Sci.*, 3(11): 289- 292.
- Goh KH, Lim TT, Dong Z (2008). Application of layered double hydroxides for the removal of oxyanions. *Water Res.*, 42(6–7): 1343–1368.
- Heidari A, Younesi H, Mehraban Z (2009). Removal of Ni (II), Cd (II) and Pb (II) from a ternary aqueous solution by amino functionalized mesoporous silica. *Chem. Eng. J.*, 153(1-3): 70-79.
- Heier LS, Meland S, Ljønes M, Salbu B, Strømseng AE (2010). Short-term temporal variations in speciation of Pb, Cu, Zn and Sb in a shooting range runoff stream. *Sci. Total Environ.*, 408(11): 2409–2417.
- Ho YS, Mackay G (2000). The kinetics of sorption of divalent metal ions onto sphagnum moss peat. *Water Res.*, 34(3): 735–742.
- Huang C, Hu B (2008). Silica-coated magnetic nanoparticles modified with  $\gamma$ - mercaptopropyltrimethoxysilane for fast and selective solid phase extraction of trace amounts of Cd, Cu, Hg and Pb in environmental and biological samples prior to their determination by inductively coupled plasma mass spectrometry. *Spectrochim. Acta B* 63(3): 437-444.
- Jayakumar R, Menon D, Manzoor K, Nair SV, Tamura H (2010). Biomedical applications of chitin and chitosan based nanomaterials-A short review. *Carbohyd. Polym.*, 82(2): 227–232.
- Kabbashi NA, Atieh MA, Al-Mamun A, Mirghami MES, Alam MDZ, Yahya N (2009). Kinetic adsorption of application of carbon nanotubes for Pb(II) removal from aqueous solution. *J. Environ. Sci.*, 21(4): 539–544.
- Kongsuwan A, Patnukao P, Pavasant P (2009). Binary component sorption of Cu (II) and Pb (II) with activated carbon from Eucalyptus camaldulensis Dehn bark. *J. Ind. Eng. Chem.*, 15(4): 465–470.
- Lalhrualtuanga H, Jayaram K, Prasad MNV, Kumar KK (2010). Lead(II) adsorption from aqueous solutions by raw and activated charcoals of *Melocanna baccifera* Roxburgh (bamboo)-A comparative study. *J. Hazard. Mater.*, 175(1–3): 311–318.
- Li CX, Gao J, Pan JM, Zhang ZL, Yan YS (2009). Synthesis, characterization, and adsorption performance of Pb(II)-imprinted polymer in nano-TiO<sub>2</sub> matrix. *J. Environ. Sci.*, 21(12): 1722–1729.
- Li KQ, Wang XH, (2009). Adsorptive removal of Pb(II) by activated carbon prepared from *Spartina alterniflora*: Equilibrium, kinetics and thermodynamics. *Bioresour. Technol.*, 100(11): 2810–2815.
- Mokhtar M, Inayat A, Ofili J, Schwieger W (2010). Thermal decomposition, gas phase hydration and liquid phase reconstruction in the system Mg/Al hydrotalcite/ mixed oxide: A comparative study. *Appl. Clay Sci.*, 50(2): 176–181.
- Naeem A, Saddique MT, Mustafa S, Kim Y, Dilara B (2009). Cation exchange removal of Pb from aqueous solution by sorption onto NiO. *J. Hazard. Mater.*, 168(1): 364–368.
- Naiya TK, Bhattacharya AK, Das SK (2009). Adsorption of Cd(II) and Pb(II) from aqueous solutions on activated alumina. *J. Colloid Interface Sci.*, 333(1): 14–26.
- Nata IF, Salim GW, Lee C (2010). Facile preparation of magnetic carbonaceous nanoparticles for  $Pb^{2+}$  ions removal. *J. Hazard. Mater.*, 183(1-3): 853-858.
- Ozay O, Ekici S, Baran Y, Aktas N, Sahiner N (2009). Removal of toxic metal ions with magnetic hydrogels. *Water Res.*, 43: 4403-4411.
- Ozdes D, Gundogdu A, Kemer B, Duran C, Senturk HB, Soyлак M (2009). Removal of Pb(II) ions from aqueous solution by a waste mud from copper mine industry: Equilibrium, kinetic and thermodynamic study. *J. Hazard. Mater.*, 166(2–3): 1480–1487.
- Özer A (2007). Removal of Pb(II) ions from aqueous solutions by sulphuric acid-treated wheat bran. *J. Hazard. Mater.*, 141(3): 753–761.
- Pronczuk J, Bruné M-N, Gore F (2011). Children's environmental health in developing countries. *Encyclopedia Environ. Health*, pp. 601–610.

- Rafatullah M, Sulaiman O, Hashim R, Ahmad A (2009). Adsorption of copper (II), chromium (III), nickel (II) and lead (II) ions from aqueous solutions by meranti sawdust. *J. Hazard. Mater.*, 170(2–3): 969–977.
- Rahmani A, Mousavi HZ, Fazli M (2010). Effect of nanostructure alumina on adsorption of heavy metals. *Desalination*, 253(1–3): 94–100.
- Reichle WT, Yang SY, Everhardt SD (1986). The nature of the thermal decomposition of a catalytically active anionic clay mineral. *J. Catal.*, 101(2): 352–359.
- Ricordel C, Darchen A, Hadjiev D (2010). Electrocoagulation-electroflotation as a surface water treatment for industrial uses. *Sep. Purif. Technol.*, 74(3): 342–347.
- Rupareila JP, Dutttagupta SP, Chatterjee AK, Mukherji S (2008). Potential of carbon nanomaterials for removal of heavy metals from water. *Desalination*, 232(1–3): 145–156.
- Singh A, Kumar D, Gaur JP (2008). Removal of Cu(II) and Pb(II) by pithophora oedogonia: sorption, desorption and repeated use of the biomass. *J. Hazard. Mater.*, 152(3): 1011–1019.
- Singh CK, Sahu JN, Mahalik KK, Mohanty CR, Mohan BR, Meikap BC (2008). Studies on the removal of Pb(II) from wastewater by activated carbon developed from Tamarind wood activated with sulphuric acid. *J. Hazard. Mater.*, 153(1–2): 221–228.
- Tao YG, Ye LB, Pan J, Wang YM, Tang B (2009). Removal of Pb(II) from aqueous solution on chitosan/TiO<sub>2</sub> hybrid film. *J. Hazard. Mater.*, 161(2–3): 718–722.
- Wang J, Zheng S, Shao Y, Liu J, Xu Z, Zhu D (2010). Amino-functionalized Fe<sub>3</sub>O<sub>4</sub>@SiO<sub>2</sub> core-shell magnetic nanomaterial as a novel adsorbent for aqueous heavy metals removal. *J. Colloid Interf. Sci.*, 349 (1): 293–299.
- Xu D, Tan XL, Chen CL, Wang XK, (2008). Removal of Pb(II) from aqueous solution by oxidized multiwalled carbon nanotubes. *J. Hazard Mater.*, 154(1–3): 407–416.
- Zhao D, Sheng G, Hu J, Chen C, Wang X (2011). The adsorption of Pb(II) on Mg<sub>2</sub>Al layered double hydroxide. *Chem. Eng. J.*, 171(1): 167–174.
- Zhang SN, Cheng FY, Tao ZL, Gao F, Chen J (2006). Removal of nickel ions from wastewater by Mg(OH)<sub>2</sub>/MgO nanostructures embedded in Al<sub>2</sub>O<sub>3</sub> membranes. *J. Alloy Compd.*, 426(1–2): 281–285.
- Zhang X, Lin S, Lu XQ, Chen ZL (2010). Removal of Pb(II) from water using synthesized kaolin supported nanoscale zero-valent iron. *Chem. Eng. J.*, 163(3): 243–248.